HHS Public Access

Author manuscript

ACS Biomater Sci Eng. Author manuscript; available in PMC 2022 January 02.

Published in final edited form as:

ACS Biomater Sci Eng. 2019 July 08; 5(7): 3595–3605. doi:10.1021/acsbiomaterials.9b00086.

Improving Sensitivity and Specificity of Amyloid-β Peptides and Tau Protein Detection with Antibiofouling Magnetic Nanoparticles for Liquid Biopsy of Alzheimer's Disease

Yuancheng Li[†,‖], **Esther Lim**[*,‡,‖], **Travis Fields**[‡], **Hui Wu**[†], **Yaolin Xu**[†], **Y. Andrew Wang**[§], **Hui Mao**[*,†]

[†] Department of Radiology and Imaging Sciences, Emory University, 1841 Clifton Road NE, Atlanta, Georgia 30329, United States

[‡] Division of Research, Philadelphia College of Osteopathic Medicine–Georgia Campus, 625 Old Peachtree Road NW, Suwanee, Georgia 30039, United States

[§] Ocean Nanotech, LLC, 7964 Arjons Drive, San Diego, California 92126, United States of America

Abstract

Alzheimer's disease (AD) is a growing global healthcare burden affecting the aging population and society. Given the lack of effective treatment to AD, early detection at the prodromal stage and timely monitoring of changes during progression are considered the best approach to control and intervene in disease progression. "Liquid biopsy" of AD biomarkers amyloid-β peptides (Aβs) and tau proteins in the cerebrospinal fluid (CSF) or blood samples holds great promises for cost-effective, widely accessible, and easy-administrated noninvasive detection and follow-up of AD. However, current *in vitro* detection methods have not yet demonstrated sufficient sensitivity and specificity using neither Aβs nor tau proteins biomarkers. One major challenge of accurate detection and measurement of biomarker levels in biofluidic samples is the biofouling effect with nonspecific adsorption of unwanted biomolecules, such as various serum proteins, on the surface of targeted detecting agents or devices, causing false-positive and false-negative findings. In this study, antibiofouling polymer polyethylene glycol-*block*-allyl glycidyl ether (PEG-*b*-AGE) coated magnetic iron oxide nanoparticles (IONPs) capable of suppressing the nonspecific interactions with biomolecules, especially proteins, were investigated for the immunomagnetic capturing of

[*] **Corresponding Authors:** hmao@emory.edu., estherli@pcom.edu.

[‖] Author Contributions

Y.L. and E.L. contributed equally. H.M., E.L., and Y.L. designed the project and formulated the experimental plan. Y.L. performed the polymer coating, ligand conjugation, and nanoparticle characterizations. Y.L. and Y.W. prepared the nanoparticles. Y.L., T.F., H.W., and Y.X. performed the detection experiments. Y.L., H.M., and E.L. analyzed the data and interpreted the results. Y.L., H.M., and E.L. were responsible for the manuscript writing. All authors have given approval to the final version of the manuscript.

The authors declare no competing financial interest.

ASSOCIATED CONTENT

Supporting Information

The Supporting Information is available free of charge on the ACS Publications website at DOI: 10.1021/acsbiomaterials.9b00086. Standard curves correlating peptide/protein concentrations (μg/mL) and fluorescence intensity from FITC or TRITC; separation efficiencies of Aβ40, Aβ42, and the tau protein from artificial CSF and FBS-added PBS by the antibody-conjugated IONPs and Dynabeads quantified by fluorescence intensity or the BCA protein assay, with or without the additions of insulin and BSA as interfering nontargeted molecules; and separation efficiencies of Aβ42 from human whole blood by anti-Aβ42 conjugated antibiofouling IONPs and anti-Aβ42 conjugated Dynabeads (PDF)

Aβ40 and Aβ42 peptides and tau protein spiked in CSF- and serum-mimicking samples using corresponding antibodies conjugated as targeting ligands. Antibody-conjugated antibiofouling IONPs demonstrated improved specificity (>90%) and sensitivity (>95%) over those of antibody-conjugated magnetic micron beads (Dynabeads, ~50% specificity and 30–40% sensitivity) widely used as magnetic separating agents under the same experimental conditions with the presence of nontargeted interfering proteins. The antibody-conjugated IONPs also exhibited significantly higher sensitivities (80–90%) and better performance of capturing Aβs and tau protein from the human whole blood samples than antibody-conjugated Dynabeads (~20%).

Graphical Abstract

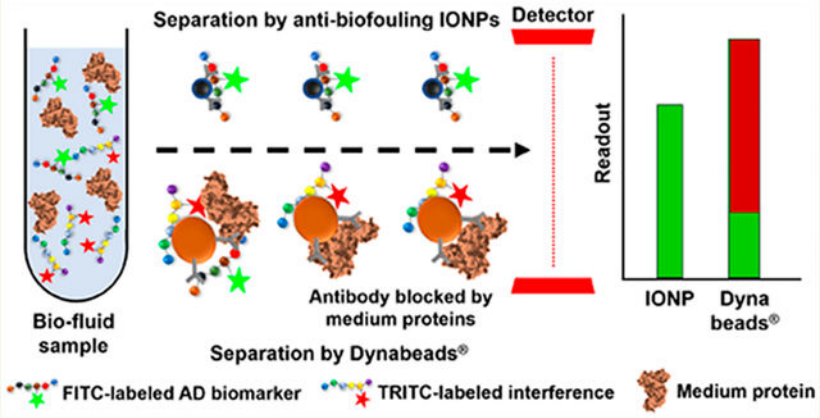

Keywords

Alzheimer’s disease; magnetic nanoparticles; amyloid-β peptides; tau proteins; immunomagnetic separation; biofouling

INTRODUCTION

Alzheimer’s disease (AD) is a major neurodegenerative disease that is commonly characterized by memory loss and cognitive decline as well as behavioral and psychological symptoms.[1] AD affects not only the patients but also the patients’ families and society. The social economic impact and healthcare burden caused by AD are rapidly growing with continuous increase of the aging population globally. While no effective treatment is currently available for AD,[2] early detection and timely monitoring of changes in the disease states are considered as the best approach to control and intervene in disease progression.[3,4] The onset of AD is widely believed to associate with the deposition of amyloid-β (Aβ), an insoluble neurotoxic polypeptide, in extracellular plaques and the aggregation of microtubule protein tau into neurofibrillary tangles in neurons.[5] Thus, the detection and quantification of levels of Aβs and tau proteins may lead to the accurate diagnosis of AD and monitoring of its progression. Positron-emission tomography (PET) imaging of Aβ deposition in the brain using a radioactive tracer, such as Pittsburgh Compound B (PiB), is currently the only clinical method for noninvasively detecting Aβs *in vivo* for confirming the AD onset.[6–8] More recently, PET imaging for tau protein aggregation has also become

available and been investigated in large cohort studies.[9] However, limited availability of imaging equipment, a complicated procedure, and the short half-time of radioisotopes make this imaging approach not cost-effective and practical for the screening and early detection of prodromal patients as well as routine monitoring of the disease with repeated scans. Therefore, various *in vitro* "liquid biopsy" tools, including those using nanomaterials and nanotechnology,[10–13]have attracted great interest for the detection of Aβs and tau proteins that spread to the peripheral blood or cerebrospinal fluid (CSF).[6–8,14] Several ultrasensitive techniques, such as surface enhanced Raman spectroscopy (SERS) and electrochemistry-based biosensors, have shown to be able to detect Aβs or tau proteins at pg/mL, and even fg/mL concentrations.[7,8,14] However, one of the major challenges in liquid biopsy is the nonspecific interactions of biological materials in the = samples with the surface of detecting agents or devices. The surface accumulation of nonspecific biomolecules, especially unwanted proteins, may interfere or attenuate the specificity of the detecting systems to the targeted biomarker molecules, causing a nonspecific background.[15–17] Such nonspecific interaction, also known as the biofouling effect, leads to adsorption of biomolecules, e.g., proteins and peptides, in biofluidic samples onto the surface of detecting agents or devices to form a layer of protein corona.[16] The protein corona may block the targeting ligands on the surface of detection agents from recognizing and binding targeted biomarkers, consequently reducing the specificity and sensitivity of biomarker targeting.[15,17] In the case of using plasma Aβ and tau protein levels to make a diagnosis of AD,[2,18,19] false-positives caused by poor specificity and false-negatives caused by poor sensitivity when attempting to detect the targeted Aβs and tau proteins from unwanted ones in the blood and CSF samples contribute to the inaccurate results.[20] In large cohort studies using Luminex xMAP technology, which are fluorometric bead-based immunoassays, to measure Aβs and tau proteins in patient plasma samples, the levels of Aβ40 and Aβ42 showed little difference between AD patients and controls,[18] while a weak correlation was observed between the higher level of the plasma tau protein concentration and dementia symptoms associated with AD.[19]

Here, we report an investigation on the biofouling effect on the sensitivity and specificity in quantitative detection of Aβ40, Aβ42, and tau protein under various conditions using immunomagnetic iron oxide nanoparticles (IONPs). We demonstrate that antibiofouling polyethylene glycol-*block*-allyl glycidyl ether (PEG-*b*-AGE) polymer coated IONPs conjugated with antibodies against Aβ40, Aβ42, and tau proteins can reduce the adsorption of nonspecific proteins while maintaining the targeting specificity to these AD biomarkers. In CSF- and human serum-mimicking conditions, the sensitivity, specificity, and efficiency of detecting Aβs and tau proteins spiked in samples by antibody-conjugated antibiofouling IONPs and widely used commercial magnetic separating agent, i.e., Dynabeads, were evaluated with the Aβ and tau protein concentrations as low as 100 ng/mL. The results demonstrated the improved detection accuracy of AD biomarkers by using antibiofouling IONPs that effectively reduced the nonspecific interactions.

EXPERIMENTAL SECTION

Materials.

Amyloid-β protein fragment (1–40) (Aβ40, catalog number A1075), anti-amyloid-β (22–35) antibody (anti-Aβ40, catalog number A3356), tau protein (tau-441, human recombinant, catalog number AG960), anti-tau antibody (anti-tau, catalog number SAB5500182), fluorescein isothiocyanate (FITC), tetramethylrhodamine (TRITC), insulin (human recombinant, catalog number 91077C), bovine serum albumin (BSA, catalog number A2058), tetrahydrofuran (THF), dimethyl sulfoxide (DMSO), and ethylenediaminetetraacetic acid (EDTA) were purchased from Sigma-Aldrich (St. Louis, MO). Amyloid-β peptide (1–42) (Aβ42, human, catalog number PP66) was purchased from EMD Millipore (Burlington, MA). Anti-amyloid-β (1–28) antibody (anti-Aβ42, catalog number 250922) was purchased from Abbiotec (San Diego, CA). Magnetic beads (Dynabeads M-450 Epoxy) was purchased from Life Technologies (Carlsbad, CA). *N*-Hydroxysulfosuccinimide (sulfo-NHS), 1-ethyl-3-(3-(dimethylamino)propyl)carbodiimide hydrochloride (EDC), micro BCA protein assay kit, slide-a-lyzer dialysis cassette (MWCO 2 000), and fetal bovine serum (FBS) were purchased from Thermo Fisher Scientific (Waltham, MA). Artificial CSF was purchased from Harvard Apparatus (Holliston, MA). Phosphate-buffered saline (PBS) was purchased from Corning (Corning, NY). Activation and coupling buffers were purchased from Ocean NanoTech (San Diego, CA). EasySep Magnet was purchased from StemCell Technologies (Vancouver, Canada). Human whole blood (~12 mL) was collected from a healthy volunteer.

Preparation and Characterization of Antibiofouling Polymer Coated IONPs.

Magnetic IONPs with a 20 nm diameter core were made from a thermodecomposition method and stabilized by oleic acids in THF. The oleic acid stabilized IONPs were then coated with antibiofouling PEG-*b*-AGE diblock copolymers via ligand exchange to replace oleic acids and dispersed in deionized water. The synthesis of antibiofouling PEG-*b*-AGE copolymer and its coating on IONPs were adapted from the protocol previously reported.[21] The amphiphilic PEG-*b*-AGE polymer consisted of a hydrophilic PEG1000 moiety to reduce nonspecific protein adsorption and a hydrophobic AGE component that collapsed onto the surface of IONPs in the aqueous phase to form a protective layer. The PEG-*b*-AGE polymer utilizes a trimethoxysilane group attached on an AGE moiety to anchor on IONPs via stable semicovalent bonding with iron and an amine group on the PEG terminal for a conjugation reaction with other molecules, such as antibodies for targeting and fluorescent dyes for optical tracking. The core sizes of IONPs before and after coating and surface functionalization were measured using transmission electron microscopy (TEM, H-7500, Hitachi, Dallas, TX). The hydrodynamic sizes and surface charges of coated IONPs were measured using a dynamic light scattering (DLS) instrument (Zetasizer Nano S90, Malvern, Westborough, MA). The averaged hydrodynamic size and zeta potential were calculated from three measurements for each sample using number-weighted statistics. Iron concentrations were determined by colorimetric spectroscopy as described in the literature.[22]

Conjugation of Targeting Antibodies to Antibiofouling IONPs.

PEG-*b*-AGE coated IONPs were conjugated with anti-Aβ and anti-tau antibodies by reactions between amine groups of PEG-*b*-AGE polymers on the surface of IONPs and carboxyl groups on antibodies via NHS/EDC coupling protocol, respectively. Briefly, antibody was added to the activation buffer (400 μL) to reach the concentration of 0.25 mg/mL. EDC and sulfo-NHS were then added to the activation buffer to reach the concentrations of 0.50 and 0.25 mg/mL, respectively. After the solution was incubated for 5 min, IONPs in the coupling buffer (600 μL, 1.5 mg Fe/mL) were added to conjugate with antibodies. The solution was then incubated for 2 h at room temperature to complete the coupling reaction. Afterward, the antibody-conjugated IONPs were purified by separating from the solution in an EasySep magnet and resuspending in water. The number of antibodies conjugated to each IONP was determined by the ratio of the protein concentration (mmol/mL) of the antibody-conjugated IONP solution to the IONP concentration (mmol/mL). The concentration of conjugated antibodies was measured by the protein assay using a microBCA protein assay kit. The IONP concentration was calculated based on the iron concentration of the solution (mmol/mL) with the assumption that IONPs were spherical with a bulk magnetite density of 5.18 g/cm^3.[21] The number of antibodies conjugated to each IONP was determined by the ratio of antibody concentration (mmol/L)/IONP concentration (mmol/L).

Conjugation of Targeting Antibodies to Dynabeads.

Dynabeads (4.5 μm in diameter) were functionalized with antibodies following the manufacturer's instructions for the comparison with antibiofouling IONPs. Dynabeads(M-450 epoxy) were resuspended by vigorous vortex for 1 min. Dynabeads suspension (0.1 mL, 4.0×10^7 beads) were transferred to a centrifuge tube and mixed with 0.9 mL of borate buffer (0.1 M). Dynabeads were washed and then separated by placing the tube in a magnet for 10 min until the beads were attached to the wall of the tube before removing the supernatant. The washed Dynabeads were resuspended in 1.0 mL of borate buffer (0.1 M). The wash-resuspension was repeated twice. To prepare antibody-conjugated beads, antibodies (0.1 mg) were added to the Dynabeads suspension (1.0 mL) and the mixture was incubated for 15 min prior to adding bovine serum albumin (BSA) until the concentration reached 0.1% (w/v). After the mixture was incubated for 24 h with gentle tilting and rotation, it was placed in the magnet for 10 min to separate the antibody-conjugated beads from the suspension. The supernatant was then aspirated followed by adding 1.0 mL of PBS supplemented with 0.1% (w/v) BSA and 2 mM EDTA to resuspend the beads. The antibody-conjugated Dynabeads were purified after washing and resuspending three times. All procedures were performed at room temperature. The number of antibodies conjugated to each Dynabead was determined by the ratio of antibody concentration (mmol/L) over Dynabeads concentration (mmol/L), where antibody was quantified by measuring the difference of protein concentrations of Dynabeads after the conjugation procedure with and without the addition of antibodies, while the molar concentration of Dynabeads was converted from their concentration (4×10^8/mL).

Fluorescent Labeling of Peptides and Proteins.

In order to quantify the detected and captured tau protein and Aβs using the optical measurement, targeted or control peptides and proteins used in determining the performance of immuno-magnetic detection and separation were labeled with the green fluorescent dye FITC (excitation at 488 nm, emission at 525 nm) or the red fluorescent dye TRITC (excitation at 557 nm, emission at 576 nm) via the coupling reaction between the isothiocyanate from FITC or TRITC and the amine group from peptides and proteins. Targeted tau protein, Aβ40 and Aβ42 were labeled with FITC, while the control peptide and protein, i.e., insulin and BSA, were labeled with TRITC. Briefly, peptides or proteins were dissolved in the carbonate buffer (500 mM, pH 9.5) at the concentration of 0.5 mg/mL. FITC or TRITC solution in DMSO (10 mg/mL) was added to the peptide/protein solution to reach the dye to peptide/protein ratio of 6:100 (w/w). The mixture was incubated for 2 h at room temperature with protection from light. Afterward, the reaction solution was injected into a Slide-A-Lyzer dialysis cassette and dialyzed against deionized water to remove unconjugated fluorescent dyes. The concentrations of purified peptides/proteins were quantified using the microBCA protein assay kit. The standard curve of the correlation between peptide/protein concentrations (μg/mL) and fluorescent intensities from FITC or TRITC was obtained by measuring the fluorescent intensities using a BioTek Synergy 2 plate-reader (BioTek Instrument, Winooski, VT) at the Aβ peptide or tau protein concentrations of 0, 0.1, 0.2, 0.5, 1.0, 2.0, 5.0, 10, 20, and 50 μg/mL (Supporting Information Figure S1).

Separation of Aβ and Tau Protein in Artificial CSF or FBS Containing PBS Buffer.

Given reported results of Aβ and tau levels in CSF and plasma varied greatly from ~100 pg/mL to >10 ng/mL for Aβ40 and from <10 pg/mL to ~1 ng/mL for the tau protein depending on the cohorts and quantification techniques,[18,19,23–28] we adopted the concentration range from 100 ng/mL to 10 μg/mL for spiking Aβs and the tau protein in the testing samples to investigate the influence of biofouling effect on the specificity and sensitivity of AD biomarker detection by the antibiofouling IONPs. FITC labeled Aβ40, Aβ42, or tau protein were dissolved in artificial CSF or PBS with FBS added (50 mg/mL) in a series of concentrations (0.1, 0.2, 0.5, 1, 2, 5, and 10 μg/mL) to mimic the human CSF and serum environment, respectively.[29] In a representative procedure, the Aβ40-containing solution (500 μL) was incubated with antibody-conjugated IONPs (at a final concentration of 0.2 mg Fe/mL) or antibody-conjugated Dynabeads (1×10^6 beads, number suggested by manufacturer's instructions) for 2 h at room temperature. The tube containing the solution was then placed in an EasySep magnet for 1 h to allow magnetic particles with captured Aβ40 to attach to the tube. The supernatant was transferred to another tube and saved for quantification of residual Aβ40. Magnetic particles were redispersed in PBS (500 μL). Fluorescent signal intensity from FITC or TRITC was measured using a BioTek Synergy 2 plate-reader with the corresponding wavelength. The separation efficiency is defined by eq 1,

$$\text{separation efficiency} = \mathrm{SI_{cap}} / \left(\mathrm{SI_{cap}} + \mathrm{SI_{super}}\right) \quad (1)$$

in which SI_{cap} is the FITC fluorescent signal intensity from Aβ40 captured by magnetic particles, and SI_{super} is the FITC signal intensity from uncaptured Aβ40 in the supernatant. To verify the accuracy of the Aβ40 level quantified using the fluorescent intensity, a microBCA protein assay kit was also used to quantify the concentration of separated peptide from the artificial CSF and its supernatant following the manufacturer's instructions.

Separation of Aβs in the Presence of Nontargeted Insulin.

To demonstrate the targeting specificity of antibody-conjugated IONPs to Aβ, insulin was chosen as a nontargeted background control to add to the solution. Insulin is a peptide hormone with a molecular weight of 5.7 kDa, which has a similar chemical structure and molecular weight to those of Aβ40 (about 4.5 kDa) and thus was selected as a negative control for testing off-target influence on the detection. The separation performance of antibody-conjugated IONPs was then compared to that of antibody-conjugated Dynabeads. As illustrated in Scheme 1, after being labeled with the fluorescent dye TRITC, insulin was mixed with equal amounts of FITC-labeled Aβ40 or Aβ42 to reach a series of total concentrations (0.2, 0.4, 1, 2, 4, 10, and 20 μg/mL) in artificial CSF or PBS with FBS added (50 mg/mL). Following same procedures described above, supernatant and resuspended magnetic particles were collected for quantification of Aβ and insulin based on the fluorescent intensity. The targeting specificity was determined by the percentage of Aβ in the total captured peptides (Aβ and insulin) calculated using eq 2,

$$\text{captured A}\beta = \frac{A\beta_{cap}}{A\beta_{cap} + A\beta_{super}} \Big/ \left(\frac{A\beta_{cap}}{A\beta_{cap} + A\beta_{super}} + \frac{\text{insulin}_{cap}}{\text{insulin}_{cap} + \text{insulin}_{super}} \right) \quad (2)$$

where Aβ_{cap} and insulin_{cap} are the fluorescent signal intensities of captured Aβ and insulin measured by FITC and TRITC, respectively, while Aβ_{super} and insulin_{super} represent the signal intensities of free Aβ and insulin in the supernatant.

Separation of Tau Protein in the Presence of Nontargeted BSA.

The separation efficiency and specificity of tau protein by antibody-conjugated IONPs were examined in artificial CSF and PBS with FBS (50 mg/mL) and BSA added as the nontargeted control. Briefly, equal amounts of FITC-labeled tau protein and TRITC-labeled BSA (0.1, 0.2, 0.5, 1, 2, 5, and 10 μg/mL, respectively) were mixed together in artificial CSF or PBS with FBS added (50 mg/mL). After tau proteins were separated following the same procedure as Aβs, the concentrations of tau protein and BSA in the supernatant and resuspension were quantified by fluorescent intensities from FTIC or TRITC. The targeting efficiency was determined using eq 2 with A$\beta_{capture}$ and $\text{insulin}_{capture}$ replaced by $\text{tau}_{capture}$ and $\text{BSA}_{capture}$ and Aβ_{super} and insulin_{super} by tau_{super} and BSA_{super}.

Separation of Aβ40, Aβ42, and Tau Protein Spiked in Human Whole Blood Sample.

FITC-labeled Aβ40 was spiked into fresh human whole blood (0.5 mL) to reach the Aβ40 concentrations of 0.1, 0.5, 2.0, and 10 μg/mL, respectively. The blood was then incubated with antibody-conjugated IONPs (at the concentration of 0.2 mg Fe/mL) or

antibody-conjugated Dynabeads (1×10^6 beads) for 2 h at room temperature. Afterward, the magnetic particles with captured Aβ40 in the blood sample were separated magnetically by placing the tube in an EasySep magnet for 1 h, followed by removing supernatant and redispersing magnetic particles in PBS (500 μL). The amounts of the captured Aβ40 (μg) was calculated based on the standard curve correlating Aβ40 concentrations and fluorescent intensity from FITC. The sensitivities of detection were defined by the ratio of captured Aβ40 over the total spiked amounts.

Statistical Analysis.

The percentages of captured and remaining Aβs, insulin, tau protein, and BSA by different capturing agents were calculated with the results presented as the mean ± standard deviation. The amounts of nonspecifically adsorbed insulin or BSA onto the surfaces of IONPs or Dynabeads were compared. A two-tail unpaired *t* test was used to determine whether the differences were significant. The level of significance was set at $P < 0.05$.

RESULTS

Characterization of Antibody-Conjugated Antibiofouling Polymer Coated IONPs and Dynabeads.

The PEG-*b*-AGE polymer that provides the antibiofouling property was synthesized and used for an IONP coating as described in our previous work.[21] TEM images showed that PEG-*b*-AGE polymer coated IONPs (with the core diameter of 20 nm) were monodispersed in the aqueous solution without any aggregation (Figure 1A). The hydrodynamic size of the polymer coated IONPs measured by DLS was 33.52 ± 2.12 nm with a narrow size distribution, indicating their good stability (Figure 1B). PEG-*b*-AGE polymer not only brings in colloidal stability and antibiofouling capability for IONPs but also introduces active $-NH_2$ groups for facile functionalization of the IONPs. The specific antibodies for Aβ40, Aβ42, and tau protein were conjugated to the IONPs, respectively, through the EDC/NHS assisted coupling reaction between the $-NH_2$ groups on IONPs and the −COOH groups on antibodies.[15,21] Successful conjugations of anti-Aβ40, anti-Aβ42, and anti-tau were confirmed by the increases in hydrodynamic diameter of IONPs. As shown in Figure 1B, hydrodynamic sizes of IONPs increased from 33.52 ± 2.12 nm to 106.91 ± 8.93, 101.45 ± 9.41, and 122.45 ± 8.26 nm with anti-Aβ40, anti-Aβ42, and anti-tau antibodies conjugated on the surface. Given the sizes of anti-Aβ40, anti-Aβ42, and anti-tau were ~150 kDa, the extent of hydrodynamic diameter increase was consistent with our previous observation on the hydrodynamic size change of PEG-*b*-AGE coated IONPs after conjugating with protein ligands.[15,21] After quantifying the protein concentration (in mmol/mL) and IONP concentration (in mmol/mL) for the antibody-conjugated IONPs, the ratio of antibody/IONP was found to be ~1.8, while the ratio for Dynabeads was ~1673.

Sensitivity of Capturing Aβs and Tau Protein by Antibiofouling IONPs and Dynabeads.

We then compared the sensitivity and specificity of Aβ and tau protein detection by IONPs with those by Dynabeads. The detection sensitivities of IONPs and Dynabeads in capturing Aβ or tau protein were first investigated in artificial CSF and FBS-containing PBS (50 mg FBS/mL PBS), which mimics the condition with the presence of serum proteins.[30] As our

study focused on investigating the impact of biofouling on the AD biomarker detection, the same concentration range was applied for Aβ40, Aβ42, and tau protein in both artificial CSF and FBS-added PBS, despite that Aβ and tau protein concentrations in CSF are generally much higher than those in serum.[2,4,5,19]

As shown in Figure 2A, anti-Aβ40 conjugated IONPs and anti-Aβ40 conjugated Dynabeads demonstrated comparable capability in capturing Aβ40 spiked in the artificial CSF, achieving the separation efficiency from 89 to 100% and 83 to 100% at different Aβ40 concentrations, respectively. The separation of tau protein by these two types of magnetic particles revealed similar results, ranging from 91 to 100% by anti-tau conjugated IONPs and 87 to 100% by anti-tau conjugated Dynabeads (Figure 2C). In the FBS-containing PBS samples, the separation sensitivity of Aβ40 by anti-Aβ40 conjugated Dynabeads was greatly reduced (46–51%,Figure 2B) compared to the conditions with no FBS (artificial CSF, Figure 2A). However, anti-Aβ40 conjugated IONPs maintained 86–97% separation rate with measurable reduction of the performance at the high Aβ40 concentrations (e.g., 86% at 10 μg/mL vs 97% at 0.2 μg/mL, $P < 0.01$). The same pattern of decreased separation efficiency for tau protein was also observed in anti-tau conjugated IONPs and anti-tau conjugated Dynabeads, with 80–95% by IONPs and 31–47% for Dynabeads (Figure 2D). The decreases in sensitivities at higher concentrations of Aβ40 spiked in the sample can be explained as the targeted specific binding of Aβ40 to the particles is limited by the number of anti-Aβ40 conjugated on the surface corresponding to the increased Aβ40 concentrations. Meanwhile, there was no significant change on the sensitivity of tau protein separation ($p > 0.05$, lowest vs highest) in artificial CSF (Figure 2C), but the decrease in separation efficiency was observed ($p < 0.01$, lowest vs highest) in FBS-added PBS (Figure 2D). Since the number of tau proteins is ~10 times less than that of Aβ40 at the same concentration (μg/mL), the ratio of tau protein/anti-tau (number/number) is less susceptible to the concentration change than that of Aβ40/anti-Aβ40, contributing to the differently affected separation efficiencies of Aβ40 (decreased) and tau protein (no significant change) by anti-tau and anti-Aβ40 conjugated IONPs at different analyte concentrations.

By comparing the performance of antibiofouling IONPs and Dynabeads in different conditions, IONPs did not show a statistically significant change in sensitivity of separating Aβ40 or the tau protein in the artificial CSF and FBS-added PBS, while Dynabeads exhibited about a 40–60% decrease in the sensitivity of separating Aβ40 or tau protein. The sample medium-dependent separation performance was also observed for anti-Aβ42 conjugated Dynabeads with separation efficiencies of 82.3–100% in artificial CSF decreasing to 43.1–56.4% in FBS-containing PBS but not for anti-Aβ42 conjugated IONPs with separation efficiencies ranging from 78.2 to 100% in artificial CSF and 83.9 to 97.8% in FBS-containing PBS in the separation of Aβ42 (Figures S4 and S5 in the Supporting Information). The reduced separation efficiency (detection sensitivity) of Dynabeads in the serum-mimicking condition can be ascribed to the surface adsorption of nonspecific proteins in FBS, which attenuated the targeting sensitivity by blocking the conjugated antibodies.[15,16]

Specificity of Capturing Aβs by Antibiofouling IONPs and Dynabeads.

Recognizing that capturing nontargeted proteins in the samples can cause false positives in detection, some techniques reported earlier have attempted to eliminate the influence from the serum proteins by pretreating the detecting agents/device with albumin.[14] However, the extent of nontargeted proteins in human CSF or serum samples that lead to false positives is difficult to measure and can be sample dependent. To assess how off-target proteins may be captured with targeted Aβs or tau proteins to cause false positives, we mixed an equal amount of FITC-labeled Aβ40 and TRITC-labeled insulin into artificial CSF and FBS-containing PBS at total peptide concentrations of 0.2, 0.4, 1.0, 2.0, 4.0, 10, and 20 μg/mL.

In the artificial CSF with total concentrations of spiked Aβ40 and insulin at 0.2 and 20 μg/mL, the anti-Aβ40 conjugated IONPs separated 98.7 and 85.2% of spiked Aβ40 with only 4.1 and 12.3% of insulin “contamination”, respectively (Figure 3A), giving a false positive rate of 4.0 and 12.6% for IONPs. For the separation of Aβ42, 100.0 and 71.4% of Aβ42 spiked in the samples were separated by anti-Aβ42 conjugated IONPs, with simultaneous capturing of 3.4 and 11.2% of insulin under the same experimental setting (Supporting Information, Figure S10), resulting in the false positive rate of 3.3 and 13.6%. The increased false positive (i.e., separating more insulin) in the medium containing the higher concentration of insulin concentration, however, is not linearly increased. Aβ40 and Aβ42 are reportedly prone to bind to proteins/peptides in blood.[31,32] With the higher concentration of Aβ40, Aβ42, and insulin, the chance of Aβ40 and Aβ42 binding insulin may increase, resulting in more insulin being detected together with Aβ40. In comparison, anti-Aβ40 conjugated Dynabeads separated 94.2 and 85.5% of spiked Aβ40 under the same conditions. However, anti-Aβ40 conjugated Dynabeads also captured 96.4 and 86.4% of spiked insulin, resulting in false positive rates of 49.9 and 49.7%, respectively (Figure 3C). Similar results of separating Aβ42 in the presence of insulin were obtained (Supporting Information, Figure S10) with false positive rates of 50.1 and 48.9%. The lack of differentiating Aβ40 and Aβ42 from insulin when using Dynabeads can be ascribed to the nonspecific adsorption of insulin onto the surface, whereas the IONPs have shown to effectively avoid nonspecific protein adsorption.[21]

In the more complex serum-mimicking conditions using FBS-added PBS (50 mg FBS/mL PBS) at total concentrations of Aβ40 and insulin at 0.2 and 20 μg/mL, anti-Aβ40 conjugated IONPs captured 96.7 and 91.3% of spiked Aβ40, whereas a significantly less amount of insulin (7.9 and 11.5%, $p < 0.001$) was captured (Figure 3B). Meanwhile, when using anti-Aβ40 conjugated Dynabeads, 36.5% of spiked Aβ40 together with 45.3% of insulin was separated when the total concentration of spiked Aβ40 and insulin was 0.2 μg/mL and 28.0% of Aβ40 along with 27.0% of insulin was captured when the total concentration of spiked Aβ40 and insulin was 20 μg/mL (Figure 3D). Under the same conditions, the false positive detection rates for IONPs were found to be 7.6 and 11.2% when the total concentration of spiked Aβ40 and insulin were 0.2 and 20 μg/mL, respectively. In comparison, the false positive detection rates for Dynabeads were 55.4 and 49.1%. Likewise, the false positive rates of Aβ42 separation using anti-Aβ42 conjugated IONPs were ranging from 2.3 to 16.2% comparing to 46.4 to 52.1% for anti-Aβ42 conjugated

Dynabeads (Supporting Information, Figure S10). When comparing the performance of IONPs and Dynabeads in different medium environments, IONPs did not show a statistically significant change in terms of the specificity of separating Aβ40 from insulin (Figure 3A,B). Meanwhile, Dynabeads demonstrated a decreased specificity of separating Aβ40 from insulin when the medium was changed from the artificial CSF to serum mimicking conditions (Figure 3C,D). This is likely due to the formation of a protein corona in the serum-mimicking conditions which blocks biomarker targeting but promotes nonspecific absorption of other molecules on the particle surface.[15,17] The abundant proteins in FBS (50 mg/mL) can accumulate on the surface of Dynabeads, limiting the anti-Aβ40 interacting and binding with Aβ40 while allowing insulin to adsorb on the surface. Since the antibiofouling coating prevents nonspecific protein adsorption on the particle surface,[21] the surface is inert to the change of different media containing proteins and other nontargeted molecules and thus less susceptible to the biofouling effect on targeted separation or detection.

Specificity of Tau Protein Separation with the Presence of Nontargeted BSA.

The capture and separation of tau protein by anti-tau conjugated IONPs and anti-tau conjugated Dynabeads were also investigated with BSA as the negative control of the nontargeted interference. The tau protein used in the study is a recombinant protein expressed in *E. coli* with the molecular weight of 45.9 kDa. BSA is a protein with the molecular weight of 66.5 kDa and a similar type of structure to those of tau protein and albumins that are commonly present in human serum. Therefore, BSA is suitable for studying the influence of nonspecific proteins in CSF- and serum-mimicking media on targeted tau protein separation.

The results showed that anti-tau conjugated Dynabeads exhibited a similar performance in capturing tau protein and BSA spiked in artificial CSF, with 78.4 and 81.7% of tau protein and 80.4 and 82.3% of BSA being captured, respectively, at total concentrations of spiked tau protein and BSA of 0.2 and 20 μg/mL (Figure 4C). In this case, the false positive detection rates were 50.6 and 50.2% at these two concentrations for anti-tau conjugated Dynabeads. Under the same conditions, anti-tau conjugated IONPs were able to capture 97.9 and 98.3% of spiked tau protein with only 2.5 and 3.2% of nonspecific BSA captured (Figure 4A). Thus, the false positive detection rates for anti-tau conjugated IONPs were only 2.5 and 3.6%, substantially lower than those of anti-tau conjugated Dynabeads. In FBS-containing PBS (50 mg/mL), the separation efficiency of spiked tau protein by anti-tau conjugated IONPs decreased to 83.6 and 85.5% with 5.7 and 5.4% detection of nontargeted BSA (Figure 4B). In comparison, anti-tau conjugated Dynabeads had much lower sensitivity and specificity to the targeted tau protein with detection of 47.7% of spiked tau protein but 37.4% of spiked BSA at a total protein concentration of 0.2 μg/mL in FBS-containing PBS. A further decrease of the performance of antitau conjugated Dynabeads was observed with 26.1% separation of tau protein and 27% separation of BSA when a total protein concentration increased to 20 μg/mL (Figure 4D).

Separation of Aβs and Tau Protein from the Whole Blood.

The composition of clinical patient samples, e.g., the CSF samples collected by lumbar puncture or blood drawn from the vein, are much more complex than the artificial CSF or

FBS-containing PBS, making the accurate measurements of Aβs or tau protein even more difficult. By spiking FITC-labeled Aβs or tau protein into the human whole blood, a blood sample with known concentrations of targeted molecules can be obtained to evaluate the performance of antibiofouling IONPs and Dynabeads in detecting Aβs or tau protein. We added FITC-labeled Aβ40, Aβ42, and tau protein into the blood at final concentrations of 0.1, 0.5, 2.0, and 10 μg/mL, respectively. Since the quantification of uncaptured Aβs or tau protein in the blood is difficult due to the autofluorescence of the blood sample, the amount of separated Aβs or tau protein was determined solely according to the standard curves describing the fluorescent intensity from FITC as a function of concentration of Aβs or tau proteins. In a typical separation procedure using Dynabeads, repeated wash steps were carried out in order to remove the nonspecifically adsorbed molecules.[6] However, in this study the IONPs and Dynabeads were not washed after separation by a magnet, so that the effect of antibiofouling materials on improving the detection of biomarker molecules can be evaluated without the changes caused by the washing procedure. It was found that 75.4–81.5% of Aβ40 spiked in the blood was captured by anti-Aβ40 conjugated IONPs. In contrast, significantly less Aβ40, i.e., 18.7–24.6, was separated by anti-Aβ40 conjugated Dynabeads ($p < 0.01$, Figure 5A). A similar pattern was observed in the separation of tau protein from the blood with 86.4–91.8% of the tau protein separated by anti-tau conjugated IONPs and 20.3–27.8% of the tau protein captured by anti-tau conjugated Dynabeads (Figure 5B). The sensitivities of Aβ40 separation by IONPs did not show a measurable difference between artificial CSF (92.3 ± 6.2%) and FBS-containing PBS (94.7 ± 3.5%) but decreased in whole blood (78.4 ± 2.5%), suggesting a more complex or higher content of interfering substances in the whole blood sample (Figure 5C). Meanwhile, the sensitivity of Aβ40 separation by anti-Aβ40 conjugated Dynabeads dropped sharply from 91.2 ± 3.6% to 32.2 ± 4.6% when the sample medium was changed from artificial CSF to FBS-containing PBS and further decreased to 21.4 ± 2.7% in the whole blood sample (Figure 5C), indicating that the performance of anti-Aβ40 conjugated Dynabeads on biomarker detection or separation is more susceptible to the presence of proteins in the samples.

For separating tau proteins, anti-tau conjugated IONPs demonstrated less than a 10% medium dependent change in sensitivity, ranging from 98.0 ± 0.5% in artificial CSF to 87.9 ± 2.9% in serum-mimicking conditions and then 88.2 ± 2.5% in whole blood. In contrary, the sensitivity of tau protein detection by anti-tau conjugated Dynabeads decreased from 82.3 ± 3.0% in artificial CSF to 34.4 ± 8.0% in FBS-spiking PBS and further dropped to 25.4 ± 3.4% in whole blood, as the compositions of sample media became more complex (Figure 5D). While the detection sensitivity of anti-tau conjugated Dynabeads was compromised in the protein-rich medium, the specificities for Aβ40 and tau protein were reduced significantly to 50% when nontargeted insulin or BSA was present in the artificial CSF and FBS-added PBS (Figure 5E,F). As comparison, anti-tau conjugated IONPs maintained specificity between 90 to 100% for Aβ40 and tau protein in the artificial CSF and FBS-spiking PBS.

DISCUSSION

The current technologies for measuring of Aβs and tau proteins in CSF and plasma, e.g., enzyme-linked immunosorbent assay (ELISA) and xMAP, do not have sufficient power to

differentiate normal aging from mild cognitive impairment (MCI) or AD. While efforts have been made to improve the sensitivity and automation by employing novel technologies, the impact of biofouling to the sensitivity and specificity of currently utilized techniques has not received much attention. Both ELISA and xMAP are immunoassays that use antibody-immobilized detecting agents/device to capture Aβs and tau proteins, which are vulnerable to the biofouling effect.

Our study showed that in the presence of interfering substances, biomarker detection by widely used Dynabeads had about ~50% of false positive results with almost half of the captured molecules unwanted. In comparison, the antibiofouling IONPs reduced false positive results to less than 10% in our investigation, indicating that the detection results obtained by IONPs are more reliable than those by Dynabeads. Considering the concentrations and variety of unwanted or nontargeted materials or molecules in real serum samples are much higher than our testing samples, it is reasonable to expect much higher false positive reports by Dynabeads when dealing with human CSF or serum samples.

The testing samples with spiked Aβ40, Aβ42, or tau protein and interfering off-target molecules, i.e., insulin or BSA, offered an experimental system to examine the detection efficiency of targeted biomarkers and the false positive signal coming from nontargeted materials. In the FBS-added PBS or human whole blood, the detection sensitivity of Aβs or tau protein by antibody-conjugated Dynabeads were significantly lower than those by antibody-conjugated IONPs, due to the nonspecifically adsorbed proteins on the surface of Dynabeads, which blocked the binding between antibodies and targeted molecules. When mimicking the low concentrations of AD biomarkers in the patient CSF and serum samples, the results revealed that the nonspecific interactions of unwanted materials with the antibody-conjugated Dynabeads resulted in high false positive result, while antibody-conjugated antibiofouling IONPs have demonstrated the capacity of inert response to the nontargeted materials and maintaining target specificity to reduce false positive findings. The developed antibiofouling coating applied to the immunomagnetic capture system provides a solution to minimize the biofouling effect from taking place in the targeted biomarker capturing system, thus enabling improved detection sensitivity and specificity.

It should be noted that the current investigation was mostly limited to three known serum biomarkers for AD, while other potential markers are emerging.[33,34] In addition, our studies focused mostly on the effect of the antibiofouling coating to the sensitivity and specificity of capturing targeted biomolecules with assumptions that these molecules maintain the same properties in CSF or serum samples. Aβs are known for different conformations, such as monomers, oligomers, and fibrils, that may be associated with different stages of disease development. Moreover, other types of ligands demonstrated targeting biomarker properties, such as single stranded DNA aptamers with high binding affinities,[35,36] can also be considered to couple with the antibiofouling IONPs to capture AD or other diease biomarker molecules. For example, lower molecular weight and structurally defined aptamers may have higher efficiency in interacting with targeted biomarker molecules due to less steric hindrance and high ligand density on the surface of antibiofouling IONPs compared to bulky antibodies. These factors may need to be further elucidated in the future studies to further improve the accuracy and efficiency of the biofluid-based detection of AD biomarkers.

CONCLUSION

We have demonstrated that by coating with the antibiofouling PEG-*b*-AGE polymer, targeting ligand conjugated IONPs achieved improved specificity and sensitivity in immunomagnetic capturing of targeted AD biomarkers, i.e., Aβs and tau protein, in human CSF- and serum-mimicking environments comparing to the commercial magnetic separating agent Dynabeads without antibiofouling capability. The antibody-conjugated IONPs also exhibited significantly higher sensitivities and better performance of capturing Aβs and tau protein from human whole blood than Dynabeads. Therefore, reported antibiofouling IONPs can improve the sensitivity and accuracy of detection of AD biomarkers in patient samples with potential to be further developed and integrated into robust, cost-effective, and widely accessible benchtop AD biomarker “liquid biopsy” detection systems.

Supplementary Material

Refer to Web version on PubMed Central for supplementary material.

Funding

This study is supported in part by NIH grants (Grants U01CA198913, R01CA154846, and R01CA202846) to H.M.

ABBREVIATIONS

AD	Alzheimer’s disease
IONP	iron oxide nanoparticle
Aβs	amyloid-β peptides
CSF	cerebrospinal fluid
MCI	mild cognitive impairment
PET	positron-emission tomography
PiB	Pittsburgh compound B
SERS	surface enhanced Raman spectroscopy
PEG-*b*-AGE	polyethylene glycol-*block*-allyl glycidyl ether
FITC	fluorescein isothiocyanate
TRITC	tetramethylrhodamine
THF	tetrahydrofuran
DMSO	dimethyl sulfoxide
EDTA	ethylenediaminetetraacetic acid
PBS	phosphate-buffered saline

FBS	fatal bovine serum
sulfo-NHS	hydroxysulfosuccinimide
EDC	1-ethyl-3-(3-(dimethylamino)propyl)carbodiimide hydrochloride
DLS	dynamic light scattering
TEM	transmission electron microscope
BSA	bovine serum albumin

REFERENCES

(1). Brookmeyer R; Johnson E; Ziegler-Graham K; Arrighi HM Forecasting the Global Burden of Alzheimer's Disease. Alzheimer's Dementia 2007, 3 (3), 186–191.

(2). Wang J; Gu BJ; Masters CL; Wang Y-J A Systemic View of Alzheimer's Disease - Insights from Amyloid-Beta Metabolism Beyond the Brain. Nat. Rev. Neurol. 2017, 13 (10), 612–623. [PubMed: 28960209]

(3). Braak H; Braak E Frequency of Stages of Alzheimer-Related Lesions in Different Age Categories. Neurobiol. Aging 1997, 18 (4), 351–357. [PubMed: 9330961]

(4). Lue L-F; Guerra A; Walker DG Amyloid Beta and Tau as Alzheimer's Disease Blood Biomarkers: Promise from New Technologies. Neurol. Ther. 2017, 6 (1), 25–36.

(5). Masters CL; Bateman R; Blennow K; Rowe C; Sperling RA; Cummings JL Alzheimer's Disease. Nat. Rev. Disease Primers 2015, 1, 15056. [PubMed: 27188934]

(6). Nakamura A; Kaneko N; Villemagne VL; Kato T; Doecke J; Dore V; Fowler C; Li Q-X; Martins R; Rowe C; Tomita T; Matsuzaki k.; Ishii K; Ishii K; Arahata Y; Iwamoto S; Ito K; Tanaka K; Masters CL; Yanagisawa K High Performance Plasma Amyloid-Beta Biomarkers for Alzheimer's Disease. Nature 2018, 554 (7691), 249–254. [PubMed: 29420472]

(7). Li S-S; Lin C-W; Wei K-C; Huang C-Y; Hsu P-H; Liu H-L; Lu Y-J; Lin S-C; Yang H-W; Ma C-CM Non-Invasive Screening for Early Alzheimer's Disease Diagnosis by A Sensitively Immunomagentic Biosenser. Sci. Rep. 2016, 6, 25155. [PubMed: 27112198]

(8). Demeritte T; Viraka Nellore B. P.; Kanchanapally R; Sinha SS; Pramanik A; Chavva SR; Ray PC Hybird Graphene Oxide Based Plasmonic-Magnetic Multifunctional Nanoplatform for Selective Separation and Label-Free Identification of Alzheimer's Disease Biomarkers. ACS Appl. Mater. Interfaces 2015, 7, 13693–13700. [PubMed: 26027901]

(9). Villemagne VL; Fodero-Tavoletti MT; Masters CL; Rowe CC Tau Imaging: Early Progress and Future Directions. Lancet Neurol. 2015, 14 (1), 114–124. [PubMed: 25496902]

(10). Elbassal EA; Morris C; Kent TW; Lantz R; Ojha B; Wojcikiewicz EP; Du D Gold Nanoparticles as a Probe for Amyloid-beta Oligomer and Amyloid Formation. J. Phys. Chem. C 2017, 121 (36), 20007–20015.

(11). Neely A; Perry C; Varisli B; Singh AK; Arbneshi T; Senapati D; Kalluri JR; Ray PC Ultrasensitive and Highly Selective Detection of Alzheimer's Disease Biomarker Using Two-Photon Rayleigh Scattering Properties of Gold Nanoparticle. ACS Nano 2009, 3 (9), 2834–2840. [PubMed: 19691350]

(12). Chou I-H; Benford M; Beier HT; Cote GL Nanofluidic Biosensing for Beta-Amyloid Detection Using Surface Enhanced Raman Spectroscopy (SERS). Nano Lett. 2008, 8 (6), 1729–1735. [PubMed: 18489171]

(13). Huang A; Zhang L; Li W; Ma Z; Shuo S; Yao T Controlled Fluorescence Quenching by Antibody-Conjugated Graphen Oixde to Measure Tau Protein. R. Soc. Open Sci. 2018, 5 (4), 171808. [PubMed: 29765647]

(14). Yoo YK; Kim J; Kim G; Kim YS; Kim HY; Lee S; Cho WW; Kim S; Lee S-M; Lee BC; Lee JH; Hwang KS A Highly Sensitive Plasma-Based Amyloid-beta Detection System through

Medium-Changing and Noise Cancellation System for Early Diagnosis of The Alzheimer's Disease. Sci. Rep. 2017, 7 (1), 8882. [PubMed: 28827785]

(15). Lin R; Li Y; MacDonald T; Wu H; Provenzale J; Peng X; Huang J; Wang L; Wang AY; Yang J; Mao H Improving Sensitivity and Specificity of Capturing and Detecting Targeted Cancer Cells with Anti-Biofouling Polymer Coated Magnetic Iron Oxide Nanoparticles. Colloids Surf., B 2017, 150 (1), 261–270.

(16). Li Y; Xu Y; Fleischer CC; Huang J; Lin R; Yang L; Mao H Impact of Anti-Biofouling Surface Coating on The Properties of Nanomaterials and Their Biomedical Applications. J. Mater. Chem. B 2018, 6 (1), 9–24. [PubMed: 29479429]

(17). Salvati A; Pitek AS; Monopoli MP; Prapainop K; Bombelli FB; Hristov DR; Kelly PM; Aberg C; Mahon E; Dawson KA Transferrin-Functionalized Nanoparticles Lose Their Targeting Capabilties When A Biomolecule Corona Adsorbs on The Surface. Nat. Nanotechnol. 2013, 8, 137–143. [PubMed: 23334168]

(18). Lovheim H; Elgh F; Johansson A; Zetterberg H; Blennow K; Hallmans G; Eriksson S Plasma Concentrations of Free Amyloid Beta Cannot Predict the Development of Alzheimer's Disease. Alzheimer's Dementia 2017, 13 (7), 778–782.

(19). Mattsson N; Zetterberg H; Janelidze S; Insel PS; Andreasson U; Stomrud E; Palmqvist S; Baker D; Tan Hehir C. A.; Jeromin A; Hanlon D; Song L; Shaw LM; Trojanowski JQ; Weiner MW; Hansson O; Blennow K Plasma Tau in Alzheimer Disease. Neurology 2016, 87 (17), 1827–1835. [PubMed: 27694257]

(20). Henriksen K; O'Bryant SE; Hampel H; Trojanowski JQ; Montine TJ; Jeromin A; Blennow K; Lonneborg A; Wyss-Coray T; Soares H; Bazenet C; Sjogren M; Hu W; Lovestone S; Karsdal MA; Weiner MW The Futrue of Blood-Based Biomarkers for Alzheimer's Disease. Alzheimer's Dementia 2014, 10 (1), 115–131.

(21). Li Y; Lin R; Wang L; Huang J; Wu H; Cheng G; Zhou Z; MacDonald T; Yang L; Mao H PEG-b-AGE Polymer Coated Magnetic Nanoparticle Probes with Facile Functionalization and Anti-Fouling Properties for Reducing Non-Specific Uptake and Improving Biomarker Targeting. J. Mater. Chem. B 2015, 3, 3591–3603. [PubMed: 26594360]

(22). Huang J; Wang L; Zhong X; Li Y; Yang L; Mao H Facile Non-Hydrothermal Synthesis of Oligoasccharides Coated Sub-5 nm Magnetic Iron Oxide Nanoparticles with Dual MRI Contrast Enhancement Effect. J. Mater. Chem. B 2014, 2 (33), 5344–5351.

(23). Toledo JB; Vanderstichele H; Figurski M; Aisen PS; Petersen RC; Weiner MW; Jack CRJ; Jagust W; Decarli C; Toga AW; Toledo E; Xie SX; Lee VM-Y; Trojanowski JQ; Shaw LM Factors Affecting Aβ Plasma Levels and Their Utility as Biomarkers in ADNI. Acta Neuropathol. 2011, 122 (4), 401–413. [PubMed: 21805181]

(24). Mehta PD; Pirttila T; Patrick BA; Barshatzky M; Mehta SP Amyloid β Protein 1–40 and 1–42 Levels in Matched Cerebrospinal Fluid and Plasma from Patients with Alzheimer Disease. Neurosci. Lett. 2001, 304 (1–2), 102–106. [PubMed: 11335065]

(25). Hanon O; Vidal J-S; Lehmann S; Bombois S; Allinquant B; Treluyer J-M; Gele P; Delmaire C; Blanc F; Mangin J-F; Buee L; Touchon J; Hugon J; Vellas B; Galbrun E; Benetos A; Berrut G; Paillaud E; Wallon D; Castelnovo G; Volpe-Gillot L; Paccalin M; Robert P-H; Godefroy O; Dantoine T; Camus V; Belmin J; Vandel P; Novella J-L; Duron E; Rigaud A-S; Schraen-Maschke S; Gabelle A Plasma Amyloid Levels within the Alzheimer's Process and Correlations with Central Biomarkers. Alzheimers Dement. 2018, 14 (7), 858–868. [PubMed: 29458036]

(26). Zetterberg H; Wilson D; Andreasson U; Minthon L; Blennow K; Randall J; Hansson O Plasma Tau Levels in Alzheimer's Disease. Alzheimer's Res. Ther. 2013, 5 (2), 9. [PubMed: 23551972]

(27). Mehta PD; Pirttila T; Mehta SP; Sersen EA; Aisen PS; Wisniewski H Plasma and Cerebrospinal Fluid Levels of Amyloid β Proteins 1–40 and 1–42 in Alzheimer Disease. Arch. Neurol. 2000, 57 (1), 100–105. [PubMed: 10634455]

(28). Fagan AM; Roe CM; Xiong C; Mintun MA; Morris JC; Holtzman DM Cerebrospinal Fluid Tau/Beta-Amyloid(42) Ratio as A Prediction of Cognitive Decline in Nondemented Older Adults. Arch. Neurol. 2007, 64 (3), 343–349. [PubMed: 17210801]

(29). Walker HK; Hall WD; Hurst JW Clinical Methods: The History, Physical, and Laboratory Examinations, 3rd ed.; Butterworths: Boston, MA, 1990.

(30). Anderson NL; Anderson NG The Human Plasma Proteome: History, Character, and Diagnostic Prospects. Mol. Cell. Proteomics 2002, 1 (11), 845–867. [PubMed: 12488461]

(31). Roher AE; Esh CL; Kokjohn TA; Castano EM; van Vickle GD; Kalback WM; Patton RL; Luehrs DC; Daugs ID; Kuo Y-M; Emmerling MR; Soares H; Quinn JF; Kaye J; Connor DJ; Silverberg NB; Adler CH; Seward JD; Beach TG; Sabbagh MN Ab Peptide in Human Plasma and Tissues and Their Significance for Alzheimer's Disease. Alzheimer's Dementia 2009, 5 (1), 18–29.

(32). Okereke OI; Xia W; Irizarry MC; Sun X; Qiu WQ; Fagan AM; Mehta PD; Hyman BT; Selkoe DJ; Grodstein F Performance Characteristics of Plasma Amyloid Beta 40 and 42 Assays. J. Alzheimer's Dis. 2009, 16 (2), 277–285. [PubMed: 19221417]

(33). Lashley T; Schott JM; Weston P; Murray CE; Wellington H; Keshavan A; Foti SC; Foiani M; Toombs J; Rohrer JD; Heslegrave A; Zetterberg H Molecular Biomarkers of Alzheimer's Disease: Progress and Prospects. Dis. Models & Mech. 2018, 11 (5), No. dmm031781.

(34). Wang MJ; Yi S; Han J.-y.; Park SY; Jang J-W; Chun IK; Kim SE; Lee BS; Kim GJ; Yu JS; Lim K; Kang SM; Park YH; Youn YC; An SSA; Kim S Oliomeric Forms of Amyloid-beta Protein in Plasma as A Potential Blood-Based Biomarker for Alzheimer's Disease. Alzheimer's Res. Ther. 2017, 9 (98), 1727.

(35). Teng I-T; Li X; Yadikar HA; Yang Z; Li L; Lyu Y; Pan X; Wang KK; Tan W Identificiation and Characterization of DNA Aptamer Specific for Phosphorylation Epitopes of Tau Protein. J. Am. Chem. Soc. 2018, 140 (43), 14314–14323. [PubMed: 30277395]

(36). Jiang K; Han L; Guo Y; Zheng G; Fan L; Shen Z; Zhao R; Shao J A Carrier-Free Dual-Drug Nanodelivery System Functionalized with Aptamer Specific Targeting HER2-Overexpressing Cancer Cells. J. Mater. Chem. B 2017, 5 (46), 9121–9129. [PubMed: 32264593]

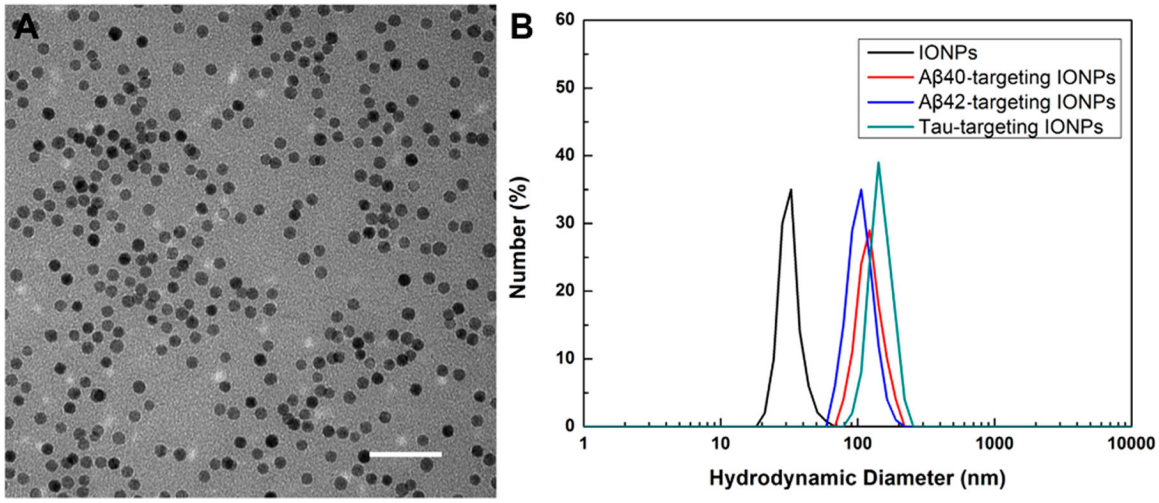

Figure 1.

(A) TEM image of PEG-*b*-AGE polymer coated IONPs (with a core diameter of 20 nm). (B) Hydrodynamic size of PEG-*b*-AGE polymer coated IONPs (black) increased after conjugation of anti-Aβ40 (red), anti-Aβ42 (blue), and anti-tau (green), suggesting the successful attachment of antibodies on the particle surface. Scale bar, 200 nm.

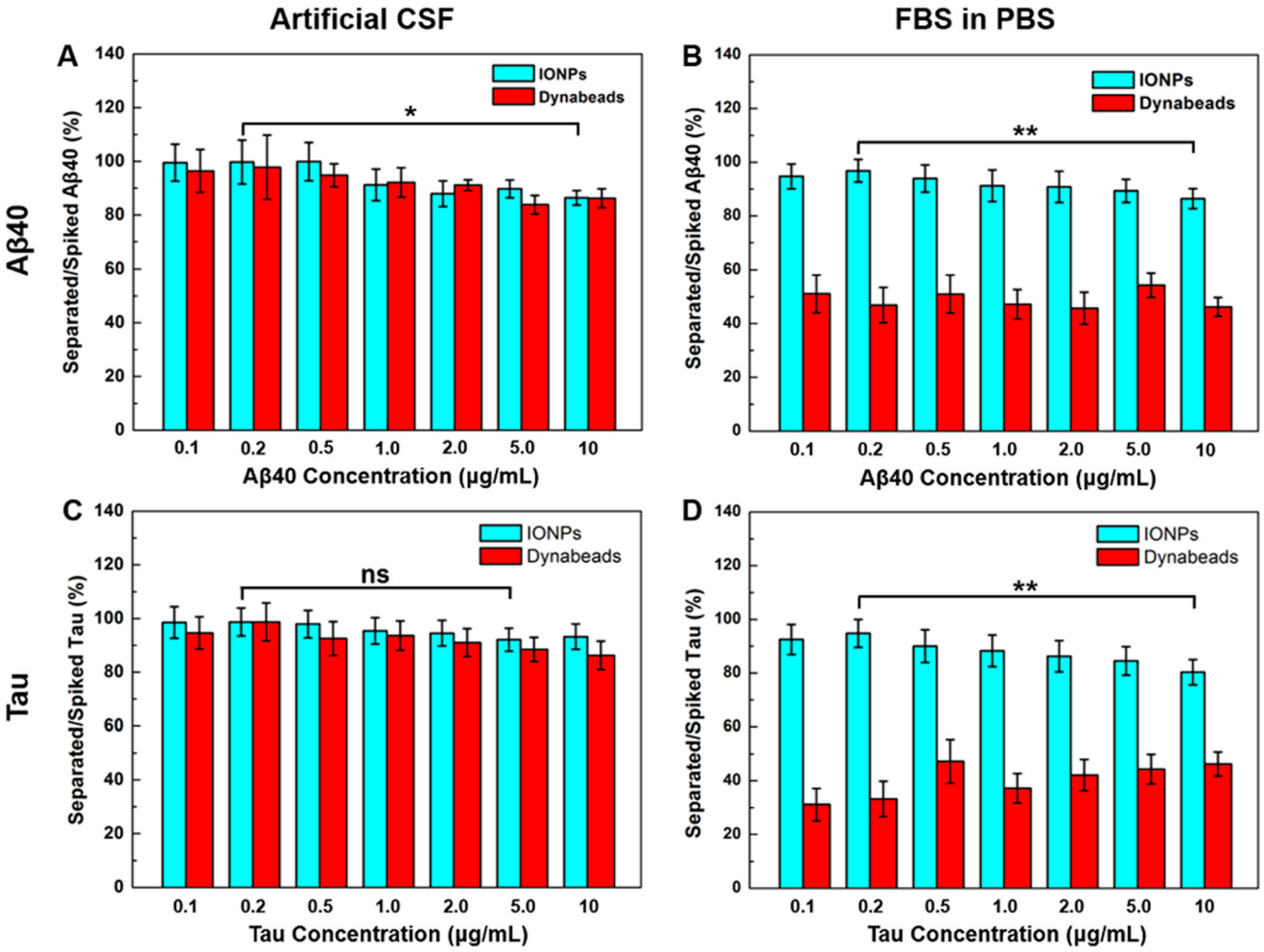

Figure 2.

Percentages of captured Aβ40 by anti-Aβ40 conjugated Dynabeads and anti-Aβ40 conjugated IONPs in total spiked Aβ40 from (A) artificial CSF and (B) FBS-containing PBS (50 mg FBS/mL PBS) with the Aβ40 spiking concentrations ranging from 0.1 to 10 μg/mL. The separation efficiencies of tau protein by anti-tau conjugated Dynabeads and anti-tau conjugated IONPs from (C) artificial CSF and (D) FBS-containing PBS. *$p < 0.05$, **$p < 0.01$.

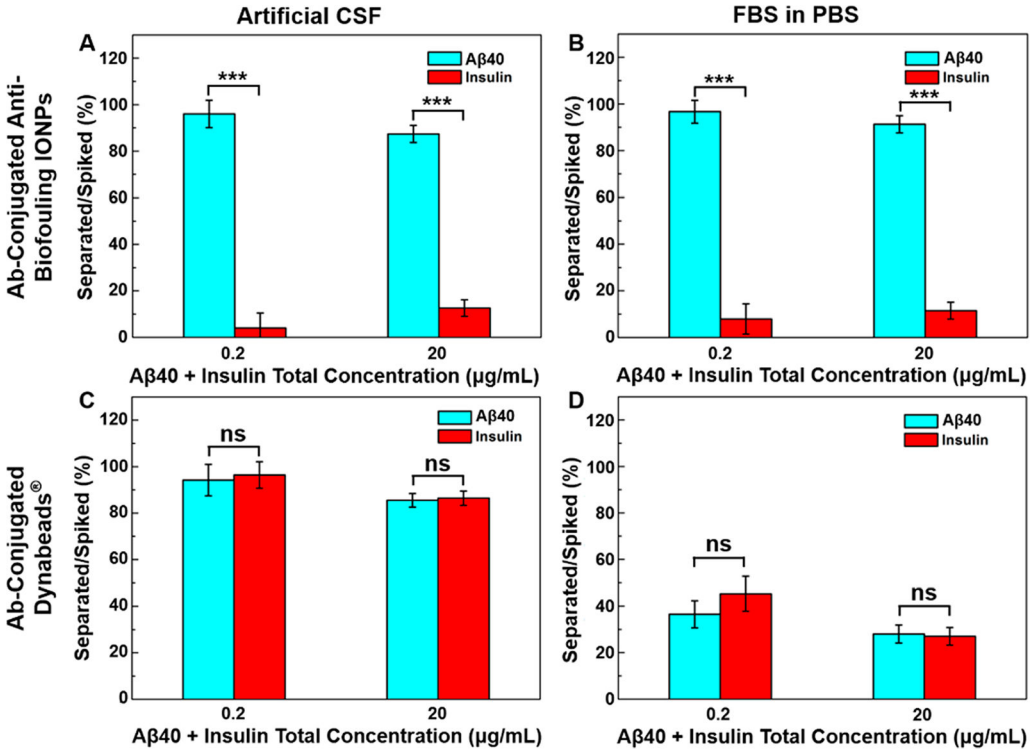

Figure 3.

Specificity of Aβ40 detection demonstrated by the separated percentage of targeted Aβ40 and nontargeted insulin at equal amounts with total concentrations of 0.2 and 20 μg/mL by anti-Aβ40 conjugated IONPs in (A) artificial CSF and (B) FBS-containing PBS (50 mg FBS/mL PBS) and by anti-Aβ40 conjugated Dynabeads in (C) artificial CSF and (D) FBS-containing PBS. ***$p < 0.001$.

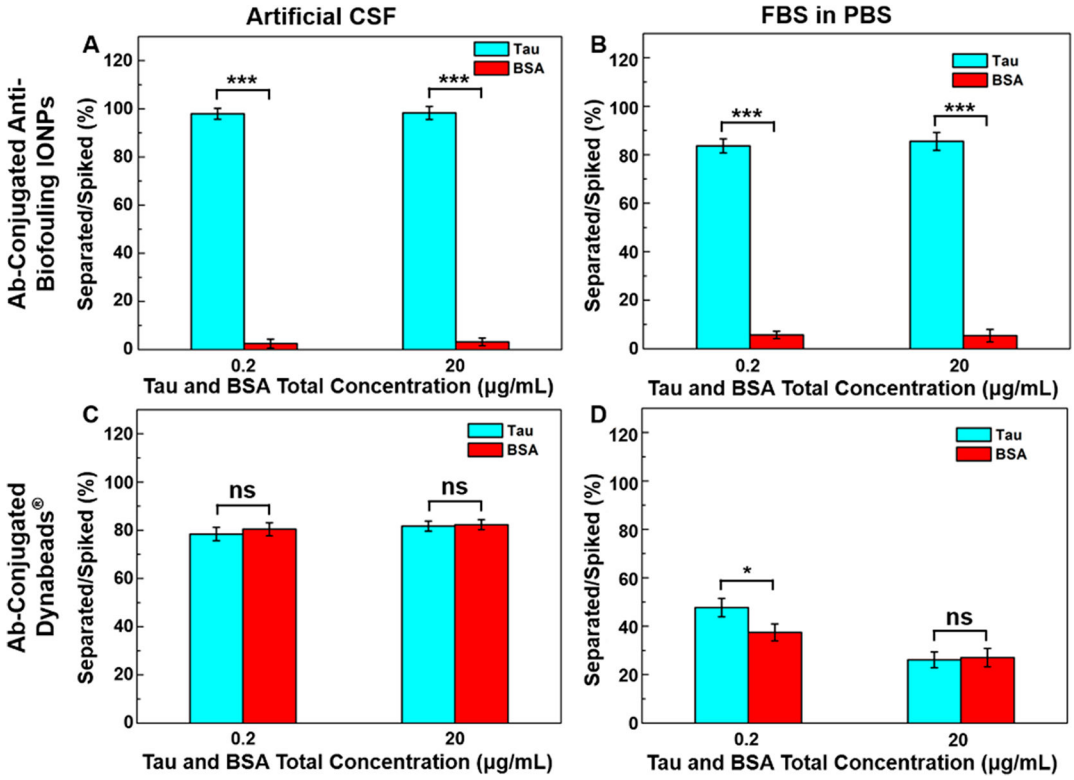

Figure 4.

Detection of the tau protein by anti-tau conjugated IONPs with equal amounts of BSA added as a nontargeted interference in tau and BSA total concentrations of 0.2 and 20 μg/mL in (A) artificial CSF and (B) FBS-containing PBS (50 mg FBS/mL PBS), and by anti-tau conjugated Dynabeads in (C) artificial CSF and (D) FBS-containing PBS. *$p < 0.05$, ***$p < 0.001$.

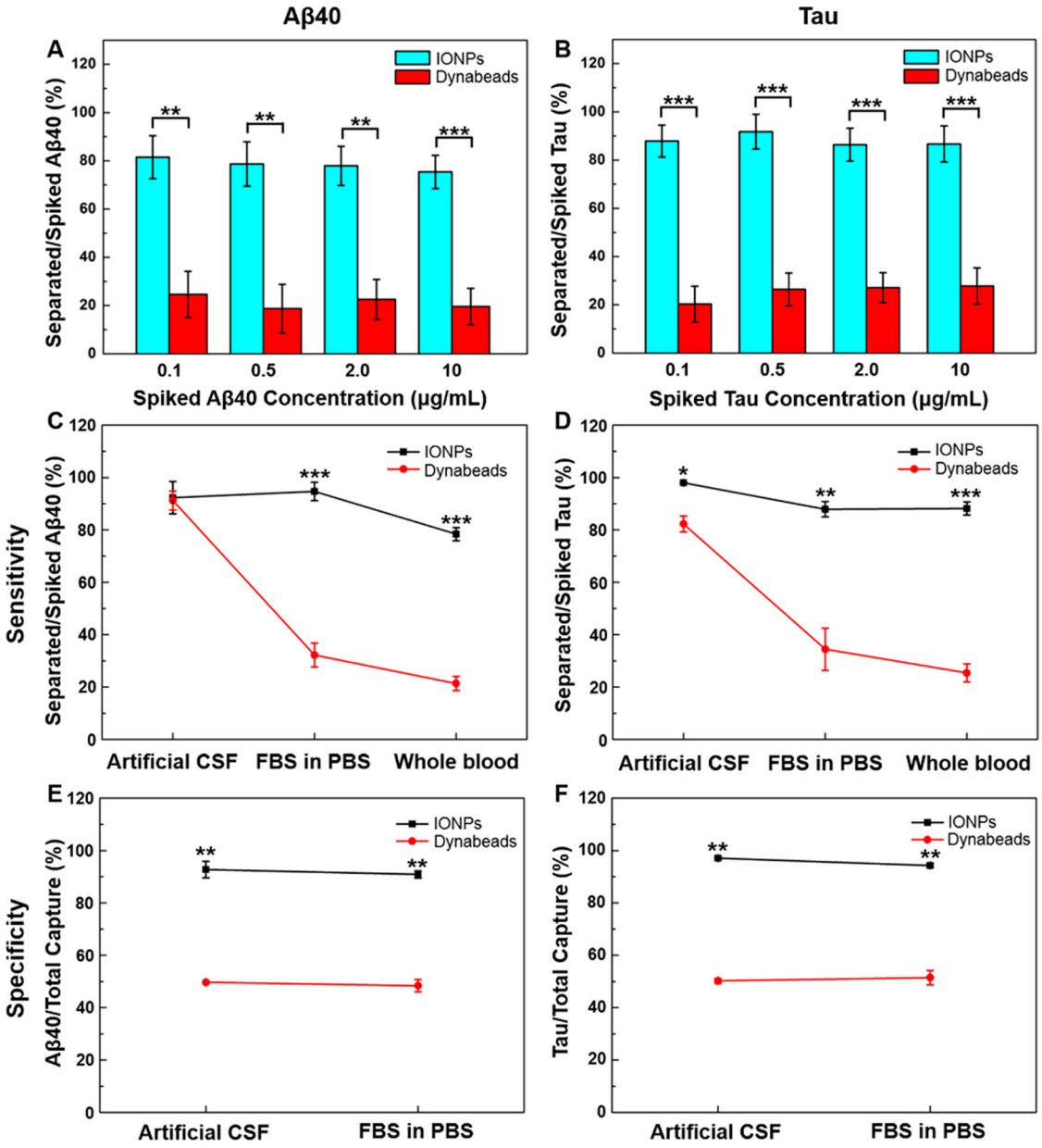

Figure 5.

(A) Aβ40 and (B) tau protein separation from human whole blood by anti-Aβ40 or anti-tau conjugated IONPs and anti-Aβ40 or anti-tau conjugated Dynabeads with Aβ40 or tau protein concentrations of 0.1, 0.5, 2.0, and 20 μg/mL. The sensitivity comparison of IONPs and Dynabeads on the separation of (C) Aβ40 and (D) tau protein in artificial CSF, FBS-containing PBS, and whole blood. The specificity of IONPs and Dynabeads on the separation of (E) Aβ40 and (F) tau protein in artificial CSF and FBS-containing PBS.

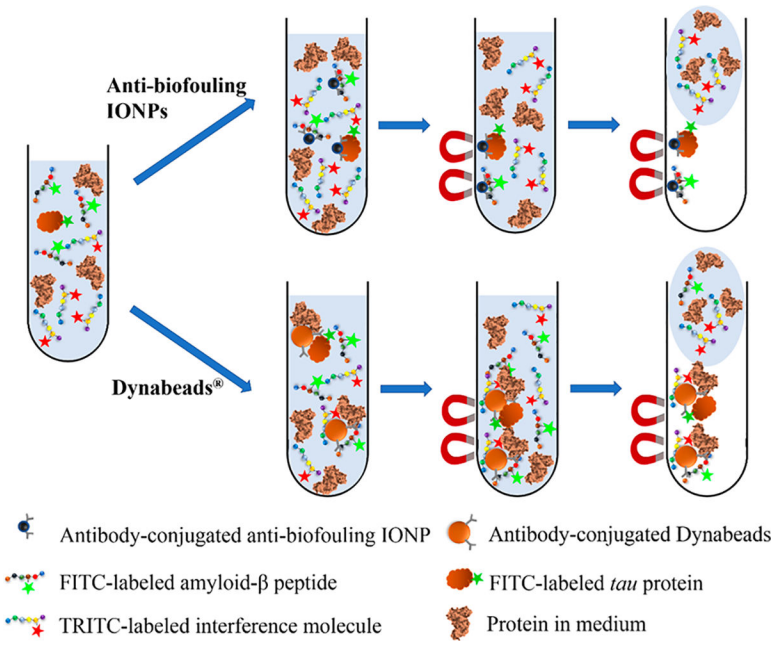

Scheme 1. Illustration of Immunomagnetic Separation of Aβs and Tau Proteins in CSF or Serum by Antibody-Conjugated IONPs or Dynabeads with the Presence of Nontargeted Interfering Molecules